

IMPLICATIONS FROM ASKAP FAST RADIO BURST STATISTICS

WENBIN LU¹ AND ANTHONY L. PIRO²

Submitted for publication in The Astrophysical Journal Letters

ABSTRACT

Although there has recently been tremendous progress in studies of fast radio bursts (FRBs), the nature of their progenitors remains a mystery. A fundamental question associated with this is the relation between FRBs that are observed to repeat and those that have only shown a single burst. We study the current FRB population to better understand their energetics and statistics. For a power-law volumetric rate per unit isotropic energy $dN/dE \propto E^{-\gamma}$, we show that the observed cumulative distribution of dispersion measure (DM) scales $N(> DM) \propto DM^{5-2\gamma}$ for $\gamma > 1$. Comparing this with the observed distribution of the ASKAP sample, we find a good fit for $\gamma \simeq 1.7$. The similarity of this value to that of repeating FRBs argues that single bursts may share the same underlying physical mechanism with the repeaters. We also discuss the fluence distribution of the ASKAP sample, which allows us to estimate a maximum isotropic burst energy of $E_{\max} \simeq 2 \times 10^{33}$ erg Hz⁻¹ as well as the volumetric rate of FRBs as a function of their energies. We provide fitting functions that can be applied to the much larger FRB samples expected in the near future to study their distributions, energetics, and rates.

Subject headings: radio continuum: general

1. INTRODUCTION

Fast radio bursts (FRBs, Lorimer et al. 2007; Thornton et al. 2013) are millisecond radio pulses with large dispersion measures (DMs) strongly suggesting an extragalactic origin. This has been directly confirmed by the repeater FRB 121102 (Spitler et al. 2016), which has been localized to a $z = 0.19$ galaxy (Chatterjee et al. 2017; Tendulkar et al. 2017). FRBs promise to provide amazing probes of the baryonic distribution across cosmological distances, but before their full potential can be reached, a fundamental understanding of their source (or sources) is required (for a summary of potential progenitor models see Platts et al. 2018)³. A chief issue is the connection between repeating FRBs and those that have only shown a single burst. Do all FRBs have the same source as the repeaters? Is so, can we apply what we learn from the repeaters to all FRBs? And how does their nature impact their utility as cosmological probes?

These questions have made discovering FRBs and measuring their physical properties some of the leading scientific goals of many current and future telescopes, such as Parkes (Thornton et al. 2013; Champion et al. 2016; Bhandari et al. 2018), Arecibo (Spitler et al. 2016), UTMOST (Bailes et al. 2017; Caleb et al. 2017), ASKAP (Bannister et al. 2017; Shannon et al. 2018), CHIME (CHIME/FRB Collaboration et al. 2018), FAST (Li et al. 2013), and Apertif (Maan & van Leeuwen 2017). This has led to a rapidly growing but highly heterogeneous sample of FRBs. In Figure 1, we summarize the DM and fluence of currently published FRBs (Petroff et al.

2016)⁴. The DMs are obtained by subtracting from the total measured values the contributions of the interstellar medium (Yao et al. 2017) and halo ($DM_{\text{halo}} = 30 \text{ pc cm}^{-3}$) of the Milky Way.

Many studies have been carried out to statistically constrain the volumetric rate and luminosity/energy distribution function of the growing sample of FRBs, which may provide important clues about their progenitors (Katz 2016; Lu & Kumar 2016; Li et al. 2017; Nicholl et al. 2017; Macquart & Ekers 2018; Luo et al. 2018). Such work has mainly focused on the Parkes sample. Although Parkes accounts for almost half of the bursts, there are many selection effects that make it fluence-incomplete (Keane & Petroff 2015; Patel et al. 2018), e.g., different backend instruments (AFB vs. BPSR) and galactic-latitude rate dependence (Petroff et al. 2014; Burke-Spolaor & Bannister 2014). Likely the most serious issue is that the fluences of Parkes bursts are often lower limits and are uncertain by as large as a factor of ~ 5 due to poor localization by single-beam detection (Ravi 2019).

Recently, the Commensal Real-time ASKAP Fast Transient (CRAFT) survey, targeting the brightest portion of the FRB population, has published 23 bursts — the first and largest well-controlled sample to date. These bursts have well-measured fluences (uncertainty⁵ of $\sim 20\%$) because the overlapping beam arrangement allows the full focal plane to be uniformly sampled (Shannon et al. 2018). The survey had high galactic latitude pointings $|b| = 50 \pm 5$ deg, which eliminates potential biases due to varying sky temperature and Galactic DM contribution. For the above reasons, we focus on the rel-

¹ TAPIR, Walter Burke Institute for Theoretical Physics, Mail Code 350-17, Caltech, Pasadena, CA 91125, USA; wenbinlu@caltech.edu

² The Observatories of the Carnegie Institution for Science, 813 Santa Barbara St., Pasadena, CA 91101, USA; piro@carnegiescience.edu

³ <http://frbtheorycat.org>

⁴ <http://frbcat.org>

⁵ One exception is FRB 170110 with a fluence of 200_{-100}^{+500} Jy ms (90% confidence). This large uncertainty is due to detection in a corner beam with poor localization (Shannon et al. 2018). Nevertheless, it is well above the ASKAP fluence threshold and is hence included in our analysis.

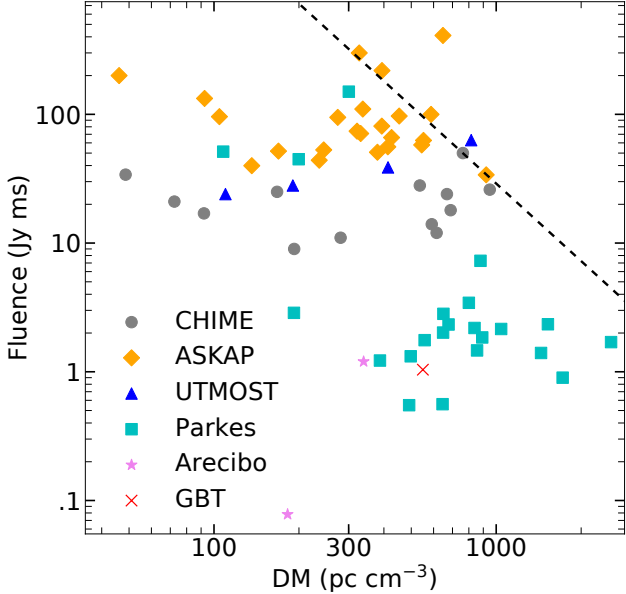


FIG. 1.— The DM and fluence of the current sample of FRBs from the FRB Catalog (Petroff et al. 2016). The dashed line shows $F = E_{\max}/4\pi D^2$ for $E_{\max} = 2 \times 10^{33} \text{ erg Hz}^{-1}$ and the relation between luminosity distance D and DM is given by Equation (9).

actively uniform ASKAP sample (Bannister et al. 2017; Shannon et al. 2018; Macquart & Ekers 2018), which appears roughly complete down to a threshold fluence of $F_{\text{th}} \sim 50 \text{ Jy ms}$.

This Letter is organized as follows. We use a simple model to explain the observed DM distribution in Section 2 and the fluence distribution in Section 3. Then, we discuss the inferred model parameters and implications in Section 4. A few potential caveats and issues to keep in mind for future work are discussed in Section 5. We conclude with a summary of this work in Section 6.

2. DM DISTRIBUTION

In our sample, bursts with similar DM (or distance) show a large spread in fluences, which motivates us to consider a power-law volumetric rate of FRB events per unit (isotropic) energy

$$\frac{dN}{dE} = AE^{-\gamma}, \quad (1)$$

with a maximum energy of E_{\max} above which there are no FRBs.

Law et al. (2017) find a power-law index of $\gamma \simeq 1.7$ from the statistics of the first repeater FRB 121102. This is similar to the energy distribution of high-energy bursts from magnetar (Turolla et al. 2015), which perhaps lends support for models which argue for magnetars as the progenitors of FRBs (Popov & Postnov 2010; Lyubarsky 2014; Kulkarni et al. 2014; Pen & Connor 2015; Katz 2016; Kumar et al. 2017; Metzger et al. 2017; Beloborodov 2017). Whether or not this is the case, such indices are natural consequences of self-regulated critical phenomena (Bak et al. 1987; Aschwanden et al. 2016).

Setting F_{th} as the threshold fluence for detection, the

total number of events observed below a distance D is

$$\begin{aligned} N(< D) &= \int_0^D 4\pi D^2 dD \int_{4\pi D^2 F_{\text{th}}}^{E_{\max}} \frac{dN}{dE} dE \\ &= \frac{AE_{\max}^{1-\gamma}}{\gamma-1} \int_0^D 4\pi D^2 dD \left[\left(\frac{4\pi D^2 F_{\text{th}}}{E_{\max}} \right)^{1-\gamma} - 1 \right]. \end{aligned} \quad (2)$$

Since bursts in our sample have low redshifts (see Figure 2), we ignored the cosmological effects and changes of the rate normalization A with distance (as would, for example, be expected if the number of FRBs scales with star formation rate).

For sufficiently nearby bursts such that $4\pi D^2 F_{\text{th}} \ll E_{\max}$, the scaling of the cumulative number is

$$N(< D) \propto \begin{cases} D^3, & \text{for } \gamma < 1, \\ D^{5-2\gamma}, & \text{for } 1 < \gamma < 5/2, \end{cases} \quad (3)$$

where the first case comes from the fact that most bursts are near E_{\max} (like standard candles) and the second case reflects the effect of a wide distribution of burst energies.

For sufficiently large D , the rise of $N(< D)$ becomes shallower, because the maximum energy E_{\max} limits the number of high-redshift bursts. The maximum distance a burst may be detected is given by

$$D_{\max} = (E_{\max}/4\pi F_{\text{th}})^{1/2}. \quad (4)$$

The integral in Equation (2) gives

$$\begin{aligned} N(< D) &= \frac{3N_{\text{tot}}}{2(\gamma-1)} \left(\frac{D}{D_{\max}} \right)^3 \\ &\quad \times \left[\left(\frac{D}{D_{\max}} \right)^{-2(\gamma-1)} - \frac{5-2\gamma}{3} \right], \end{aligned} \quad (5)$$

where the normalization $N_{\text{tot}} = N(< D_{\max})$ is

$$N_{\text{tot}} = \frac{2AE_{\max}^{1-\gamma}}{5-2\gamma} \frac{4\pi D_{\max}^3}{3}. \quad (6)$$

Since at low redshifts we roughly have $D \propto z \propto \text{DM}$, Equation (5) can easily be generalized as a function of z/z_{\max} or $\text{DM}/\text{DM}_{\max}$. In Figure 2, we compare the expression in Equation (5) to our ASKAP sample. We assume that the ASKAP sample is roughly complete above fluence $F_{\text{th}} = 50 \text{ Jy ms}$ (see Section 3), which encompasses 20 out of 23 bursts in the ASKAP sample (thus we take $N_{\text{tot}} = 20$). The power-law index of the energy distribution is taken to be $\gamma = 1.7$, resulting in $N(< \text{DM}) \propto \text{DM}^{1.6}$ for in low DM end.

The similarity between observed distribution and Equation (5) strongly argues that FRB sources universally share the same energy distribution as the repeater FRB 121102 even if they may only generate single bursts (see James et al. 2019; Caleb et al. 2019, for constraints on the repeating rate). This may further suggest that the underlying mechanism is similar in both the repeaters and non-repeaters. We also include a comparison to $N(< \text{DM}) \propto \text{DM}^3$ (short-dashed blue line), which is appropriate if most bursts have characteristic energy ($\gamma < 1$). This is inconsistent with the ASKAP distribution, as mentioned by Li et al. (2019).

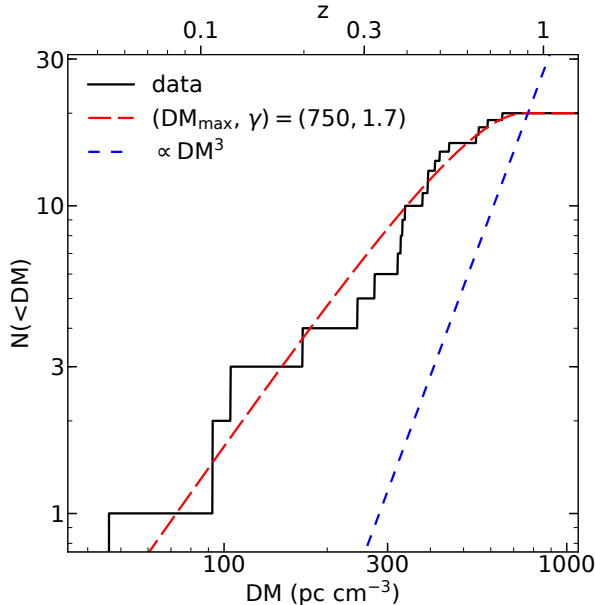


FIG. 2.— Comparison of the ASKAP FRB sample (black solid line) with Equation (5) (red dashed line) with $N_{\text{tot}} = 20$, $\text{DM}_{\text{max}} = 750 \text{ pc cm}^{-3}$, and $\gamma = 1.7$. We have subtracted the DM contributions from the Galactic interstellar medium (Yao et al. 2017) and the Galactic halo $\text{DM}_{\text{halo}} = 30 \text{ pc cm}^{-3}$. Another case of $N(< D) \propto \text{DM}^3$ is shown as a short-dashed blue line.

3. FLUENCE DISTRIBUTION

The total number of events above a measured fluence is given by

$$N(> F) = \int_0^{\sqrt{\frac{E_{\text{max}}}{4\pi F}}} 4\pi D^2 dD \int_{4\pi D^2 F}^{E_{\text{max}}} \frac{dN}{dE} dE. \quad (7)$$

Evaluating this integral and substituting the expression for D_{max} from Equation (4) and A from Equation (6), we obtain

$$N(> F) = N_{\text{tot}} \left(\frac{F}{F_{\text{th}}} \right)^{-3/2}. \quad (8)$$

Thus we expect the fluence distribution to be insensitive to γ (assuming $\gamma < 5/2$) and basically given by the value expected from a characteristic burst energy and Euclidean space. This is because, for Euclidean space, the number of bursts above a certain fluence F is dominated by those at the distance $D = \sqrt{E_{\text{max}}/4\pi F}$ where the brightest bursts are detectable (Macquart & Ekers 2018).

In Figure 3, we compare our fluence distribution given by Equation (8) with the ASKAP sample. A model with $N_{\text{tot}} = 20$ and $F_{\text{th}} = 50 \text{ Jy ms}$ provides a good fit. The sample is incomplete below the sensitivity threshold F_{th} .

4. CONSTRAINTS ON THE ENERGY DISTRIBUTION

Combining N_{tot} with DM_{max} and F_{th} estimated in the previous discussions allows us to constrain the energy distribution function of the FRB population. To relate luminosity distance and DM we use

$$D \simeq 6.7 \left(\frac{\text{DM}}{855 \text{ pc cm}^{-3}} \right) \text{ Gpc}, \quad (9)$$

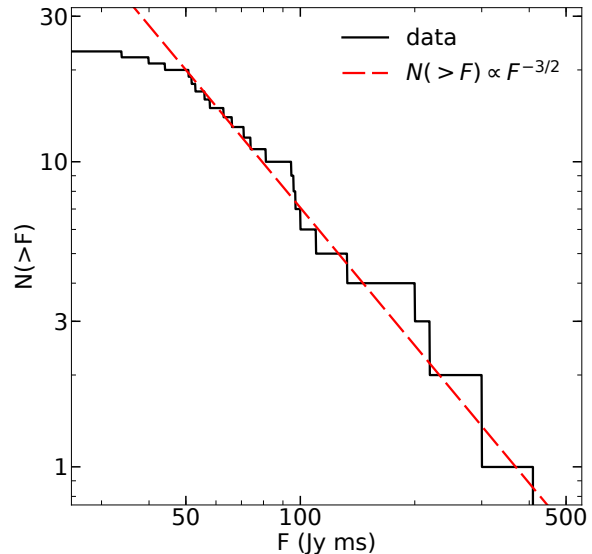


FIG. 3.— Comparison of the ASKAP FRB sample (solid black line) with Equation (8) (dashed red line) using $N_{\text{tot}} = 20$ and $F_{\text{th}} = 50 \text{ Jy ms}$. The sample is incomplete below the sensitivity threshold F_{th} .

which is scaled to match the DM given by Zhang (2018) based on the most recent Planck ΛCDM cosmology (Planck Collaboration et al. 2016). From the comparisons given in Figures 2 and 3, we can estimate the maximum isotropic FRB energy by using Equation (4),

$$E_{\text{max}} \simeq 2 \times 10^{33} \text{ erg Hz}^{-1} \frac{F_{\text{th}}}{50 \text{ Jy ms}} \left(\frac{\text{DM}_{\text{max}}}{750 \text{ pc cm}^{-3}} \right)^2 \quad (10)$$

As a greater sample of FRBs is collected, and with a better understanding of the DM_{max} within which the sample is complete and the threshold fluence of a given observatory, then E_{max} can be better measured. This in turn should be an important constraint on any emission model for FRBs (e.g., Lu & Kumar 2018). In Figure 1, we plot $F = E_{\text{max}}/4\pi D^2$ (dashed line) using the E_{max} found here. This shows that the data strongly supports this rough estimate of E_{max} with the exception of one outlier that we discuss in Section 5.

On the other hand, the total exposure of the ASKAP survey was $\Omega T \simeq 5.1 \times 10^5 \text{ deg}^2 \text{ hr}$ (Shannon et al. 2018), which can be converted to an all-sky rate of 38.8 day^{-1} above the fluence threshold $F_{\text{th}} \simeq 50 \text{ Jy ms}$. Since some bursts in our sample have moderate redshifts $z \sim 0.8$, we replace the Euclidean volume $4\pi D_{\text{max}}^3/3$ in Equation (6) with the comoving volume given by the Planck cosmology (Planck Collaboration et al. 2016). For our fiducial values $N_{\text{tot}} = 20$, $\text{DM}_{\text{max}} \simeq 750 \text{ pc cm}^{-3}$, and $\gamma \simeq 1.7$, the volumetric rate normalization is estimated to be

$$AE_{\text{max}}^{1-\gamma} \simeq 90 \text{ Gpc}^{-3} \text{ yr}^{-1}. \quad (11)$$

Taking $E_{\text{max}} \simeq 2 \times 10^{33} \text{ erg Hz}^{-1}$, we can further estimate the volumetric rate of FRBs above energy $E = 10^{30} E_{30} \text{ erg Hz}^{-1}$,

$$N(> E) \simeq \frac{AE^{1-\gamma}}{\gamma - 1} \simeq 2.7 \times 10^4 E_{30}^{-0.7} \text{ Gpc}^{-3} \text{ yr}^{-1}. \quad (12)$$

This rate density should also be an important constraint on FRB models. For a typical spectral width of $\Delta\nu = 1$ GHz, we see that the rate of FRBs with isotropic energy $> 10^{39}$ erg is roughly 10% of the core-collapse rate (Li et al. 2011; Kulkarni et al. 2014) in the local Universe. Therefore, non-repeating models based on rare events, such as long gamma-ray bursts or binary neutron star mergers (Totani 2013; Zhang 2014; Wang et al. 2016), can at most contribute a small fraction of the FRB population and are hence disfavored.

5. DISCUSSION

We note a few caveats of our work, discuss how this analysis can be generalized for larger FRB samples, and highlight some implications of our study.

(1) Instead of taking $F_{\text{th}} = 50$ Jy ms, we have also tested a more conservative choice of fluence threshold $F_{\text{th}} = 60$ Jy ms (which includes 15 out of the 23 bursts) and found that our model still provides a good fit to the DM and fluence distributions (with a slightly lower DM_{max}).

(2) We have assumed that the DM excess (beyond the Milky Way contribution) is largely due to the intergalactic medium and hence can be used as a distance indicator. However, as we know from FRB 121102 (Tendulkar et al. 2017), the host galaxy and the circum-burst medium may contribute significant fraction of DM. Unfortunately, the properties of FRB host galaxies are still highly uncertain. We also tried subtracting a constant host-galaxy contribution of 30 pc cm^{-3} , and the resulting distribution $N(< \text{DM})$ becomes slightly shallower on the low-DM end. Thus, with a larger FRB sample in the future, it is possible to constrain the (averaged) host-galaxy and circum-burst DM (e.g., from a supernova remnant, Connor et al. 2016; Piro 2016; Piro & Burke-Spolaor 2017; Piro & Gaensler 2018) by studying the deviation of the DM distribution from a power-law on the low-DM end. On the other hand, FRBs at $z \gtrsim 0.8$ may randomly have their sight lines intersecting with a few galactic haloes (McQuinn 2014; Prochaska & Zheng 2019). This effect causes stochastic deviation of the DM distribution from our model.

(3) In Figure 1, there is an outlier (FRB 180110) with inferred energy higher than E_{max} in Equation (10) by a factor of 5. A more realistic energy distribution function may have an exponential drop above the maximum energy (instead of an abrupt cutoff in our simple model). In this case, a small fraction bursts may have energies up to a few times higher than E_{max} . Alternatively, this outlier may have a large DM contribution from a combination of its host galaxy, local circum-burst environment, and intervening haloes. Magnification by plasma lensing is also a possibility (Cordes et al. 2017), although the fact that most FRBs adhere to the limit we derive argues that such effects are small in most cases.

(4) The scaling in Equation (8) breaks down at sufficiently small fluences because most bursts would come from very high redshift where the spacetime is no-longer Euclidean (the co-moving volume increases much slower than D^3) and there could be strong redshift evolution of the rate normalization $A(z)$. Although our low-redshift sample is not strongly affected by these effects, we point out the qualitative behavior for a future survey with better sensitivity.

For instance, if $A(z)$ follows the cosmic star formation rate which peaks around $z \simeq 2$, then $N(> F)$ is no longer dominated by the brightest bursts at fluence $F \ll E_{\text{max}}/4\pi D^2(z=2) \simeq 6.5 \text{ Jy ms } E_{\text{max},33.3}$, where D is the luminosity distance and $E_{\text{max},33.3} = E_{\text{max}}/10^{33.3} \text{ erg Hz}^{-1}$. In this low fluence regime, Equation (7) should be rewritten as

$$N(> F) \simeq \int_0^2 dz \frac{dV}{dz} \frac{A(z)}{1+z} \int_{4\pi D^2(z)F}^{E_{\text{max}}} E^{-\gamma} dE \quad (13)$$

$$= \frac{E_{\text{max}}^{1-\gamma}}{\gamma-1} \int_0^2 dz \frac{dV}{dz} \frac{A(z)}{1+z} \left[\left(\frac{4\pi D^2(z)F}{E_{\text{max}}} \right)^{1-\gamma} - 1 \right],$$

where dV/dz is the differential comoving volume. For $\gamma > 1$ (as indicated by the DM distribution), the integral gives $N(> F) \propto F^{1-\gamma}$, which means that a sensitive telescope with fluence threshold $F_{\text{th}} \ll 6.5 \text{ Jy ms } E_{\text{max},33.3}$ can directly measure the energy distribution slope γ by source counting. This may explain the difference in $\log N$ - $\log F$ slopes given by the Parkes and ASKAP samples (James et al. 2019), since the former has a much lower fluence threshold. In the future, with a much larger (well-controlled) sample down to a lower fluence threshold, it is possible to constrain the redshift evolution of FRB rate $A(z)$ (Macquart & Ekers 2018), which will in turn constrain the progenitor models for FRBs.

(5) The first repeater has been localized to a metal poor star-forming dwarf galaxy, suggesting that there is some relation to a long gamma-ray bursts and superluminous supernovae (Metzger et al. 2017). As more FRBs are localized, an important constraint to the progenitor model will be how much variety is seen in the hosts.

If, for example, some FRBs are found to have distinct hosts from others, one might conclude that they have different progenitors. If the distributions of the various FRB populations continue to obey similar energy distributions and maximum energies as we describe here, it argues that the underlying source is the same even if the situation that generated the source is different. For instance, in the magnetar picture, one could imagine magnetars generated both from young massive stars and old stellar environments by neutron star or white dwarf mergers. FRBs from these two populations could vary in a number of ways, from the host galaxies, to the local DM, to the rotation measure and presence of a persistent radio source. But by looking at the burst statistics as we describe here, we may understand if the underlying source is the same.

6. SUMMARY

This work suggests that when a relatively homogeneous sample of FRBs is considered, they are well described with an energy distribution with the same power-law slope as the repeating source FRB 121102, $\gamma = -d\log N/d\log E \simeq 1.7$ (Law et al. 2017), independent of whether they individually repeat themselves. This is because the observed DM distribution scales as $N(> \text{DM}) \propto \text{DM}^{5-2\gamma}$ for $\gamma > 1$.

We find that the FRB population has a maximum specific energy of $E_{\text{max}} \simeq 2 \times 10^{33} \text{ erg Hz}^{-1}$. For a spectral width of $\Delta\nu = 1$ GHz, this implies a maximum isotropic energy of order 10^{42} erg or luminosity of order $10^{45} \text{ erg s}^{-1}$ for millisecond duration, which is a factor of

a few to ten higher than that found by Luo et al. (2018) from the Parkes sample. From the total survey exposure of the ASKAP survey, we further infer a local volumetric rate of $N(> E) \simeq 2.7 \times 10^4 E_{30}^{-0.7} \text{Gpc}^{-3} \text{yr}^{-1}$ for FRBs above a specific energy $E = 10^{30} E_{30} \text{erg Hz}^{-1}$.

The existence of a maximum energy E_{max} causes the observed fluence distribution to be $N(> F) \propto F^{-3/2}$ at high fluences, because the number of bursts is dominated by those at distances $D \sim \sqrt{E_{\text{max}}/4\pi F}$. At sufficiently low fluences, the distribution approaches $N(> F) \propto F^{1-\gamma}$, reflecting the intrinsic energy distribution.

The transition between these two regimes is sensitive to the evolution of FRB rate with redshift.

Our fitting functions (Equations 5 and 7) can be directly applied to the brightest portion of other FRB samples in the near future. It is also straightforward to generalize our model to include cosmological effects and then to study how the burst distribution, energetics, and rates evolve with redshift.

WL is supported by the David and Ellen Lee Fellowship at Caltech.

REFERENCES

- Aschwanden, M. J., Crosby, N. B., Dimitropoulou, M., et al. 2016, *Space Sci. Rev.*, 198, 47
- Bailes, M., Jameson, A., Flynn, C., et al. 2017, *Publications of the Astronomical Society of Australia*, 34, e045
- Bak, P., Tang, C., & Wiesenfeld, K. 1987, *Phys. Rev. Lett.*, 59, 381
- Bannister, K. W., Shannon, R. M., Macquart, J. P., et al. 2017, *ApJ*, 841, L12
- Beloborodov, A. M. 2017, *ApJ*, 843, L26
- Bhandari, S., Keane, E. F., Barr, E. D., et al. 2018, *MNRAS*, 475, 1427
- Burke-Spolaor, S., & Bannister, K. W. 2014, *ApJ*, 792, 19
- Caleb, M., Stappers, B. W., Rajwade, K., & Flynn, C. 2019, *MNRAS*, 484, 5500
- Caleb, M., Flynn, C., Bailes, M., et al. 2017, *MNRAS*, 468, 3746
- Champion, D. J., Petroff, E., Kramer, M., et al. 2016, *MNRAS*, 460, L30
- Chatterjee, S., Law, C. J., Wharton, R. S., et al. 2017, *Nature*, 541, 58
- CHIME/FRB Collaboration, Amiri, M., Bandura, K., et al. 2018, *ApJ*, 863, 48
- Connor, L., Sievers, J., & Pen, U.-L. 2016, *MNRAS*, 458, L19
- Cordes, J. M., Wasserman, I., Hessels, J. W. T., et al. 2017, *ApJ*, 842, 35
- James, C. W., Ekers, R. D., Macquart, J. P., Bannister, K. W., & Shannon, R. M. 2019, *MNRAS*, 483, 1342
- Katz, J. I. 2016, *ApJ*, 826, 226
- Keane, E. F., & Petroff, E. 2015, *MNRAS*, 447, 2852
- Kulkarni, S. R., Ofek, E. O., Neill, J. D., Zheng, Z., & Juric, M. 2014, *ApJ*, 797, 70
- Kumar, P., Lu, W., & Bhattacharya, M. 2017, *MNRAS*, 468, 2726
- Law, C. J., Abruzzo, M. W., Bassa, C. G., et al. 2017, *ApJ*, 850, 76
- Li, D., Nan, R., & Pan, Z. 2013, in *IAU Symposium, Vol. 291, Neutron Stars and Pulsars: Challenges and Opportunities after 80 years*, ed. J. van Leeuwen, 325–330
- Li, D., Yalinewich, A., & Breyse, P. C. 2019, arXiv e-prints
- Li, L.-B., Huang, Y.-F., Zhang, Z.-B., Li, D., & Li, B. 2017, *Research in Astronomy and Astrophysics*, 17, 6
- Li, W., Chornock, R., Leaman, J., et al. 2011, *MNRAS*, 412, 1473
- Lorimer, D. R., Bailes, M., McLaughlin, M. A., Narkevic, D. J., & Crawford, F. 2007, *Science*, 318, 777
- Lu, W., & Kumar, P. 2016, *MNRAS*, 461, L122
- . 2018, *MNRAS*, L198
- Luo, R., Lee, K., Lorimer, D. R., & Zhang, B. 2018, *MNRAS*, 481, 2320
- Lyubarsky, Y. 2014, *MNRAS*, 442, L9
- Maan, Y., & van Leeuwen, J. 2017, arXiv e-prints, arXiv:1709.06104
- Macquart, J. P., & Ekers, R. 2018, *MNRAS*, 480, 4211
- McQuinn, M. 2014, *ApJ*, 780, L33
- Nitzlger, B. D., Berger, E., & Margalit, B. 2017, *ApJ*, 841, 14
- Nicholl, M., Williams, P. K. G., Berger, E., et al. 2017, *ApJ*, 843, 84
- Patel, C., Agarwal, D., Bhardwaj, M., et al. 2018, *ApJ*, 869, 181
- Pen, U.-L., & Connor, L. 2015, *ApJ*, 807, 179
- Petroff, E., van Straten, W., Johnston, S., et al. 2014, *ApJ*, 789, L26
- Petroff, E., Barr, E. D., Jameson, A., et al. 2016, *PASA*, 33, e045
- Piro, A. L. 2016, *ApJ*, 824, L32
- Piro, A. L., & Burke-Spolaor, S. 2017, *ApJ*, 841, L30
- Piro, A. L., & Gaensler, B. M. 2018, *ApJ*, 861, 150
- Planck Collaboration, Ade, P. A. R., Aghanim, N., et al. 2016, *A&A*, 594, A13
- Platts, E., Weltman, A., Walters, A., et al. 2018, arXiv e-prints
- Popov, S. B., & Postnov, K. A. 2010, in *Evolution of Cosmic Objects through their Physical Activity*, ed. H. A. Harutyunian, A. M. Mickaelian, & Y. Terzian, 129–132
- Prochaska, J. X., & Zheng, Y. 2019, *MNRAS*, 258
- Ravi, V. 2019, *MNRAS*, 482, 1966
- Shannon, R. M., Macquart, J. P., Bannister, K. W., et al. 2018, *Nature*, 562, 386
- Spitler, L. G., Scholz, P., Hessels, J. W. T., et al. 2016, *Nature*, 531, 202
- Tendulkar, S. P., Bassa, C. G., Cordes, J. M., et al. 2017, *ApJ*, 834, L7
- Thornton, D., Stappers, B., Bailes, M., et al. 2013, *Science*, 341, 53
- Totani, T. 2013, *Publications of the Astronomical Society of Japan*, 65, L12
- Turolla, R., Zane, S., & Watts, A. L. 2015, *Reports on Progress in Physics*, 78, 116901
- Wang, J.-S., Yang, Y.-P., Wu, X.-F., Dai, Z.-G., & Wang, F.-Y. 2016, *ApJ*, 822, L7
- Yao, J. M., Manchester, R. N., & Wang, N. 2017, *ApJ*, 835, 29
- Zhang, B. 2014, *ApJ*, 780, L21
- . 2018, *ApJ*, 867, L21